

# Impacts of 319 wind farms on surface temperature and vegetation in the United States

Yingzuo Qin, Yan Li, Ru Xu, Chengcheng Hou, Alona Armstrong, Eviatar Bach, Yang Wang, Bojie Fu

▶ **To cite this version:**

Yingzuo Qin, Yan Li, Ru Xu, Chengcheng Hou, Alona Armstrong, et al.. Impacts of 319 wind farms on surface temperature and vegetation in the United States. Environmental Research Letters, 2022, 17, 10.1088/1748-9326/ac49ba . insu-03610734

**HAL Id: insu-03610734**

**https://insu.hal.science/insu-03610734**

Submitted on 16 Mar 2022

**HAL** is a multi-disciplinary open access archive for the deposit and dissemination of scientific research documents, whether they are published or not. The documents may come from teaching and research institutions in France or abroad, or from public or private research centers.

L'archive ouverte pluridisciplinaire **HAL**, est destinée au dépôt et à la diffusion de documents scientifiques de niveau recherche, publiés ou non, émanant des établissements d'enseignement et de recherche français ou étrangers, des laboratoires publics ou privés.



Distributed under a Creative Commons Attribution 4.0 International License

ENVIRONMENTAL RESEARCH
LETTERS

LETTER • OPEN ACCESS

# Impacts of 319 wind farms on surface temperature and vegetation in the United States

To cite this article: Yingzuo Qin *et al* 2022 *Environ. Res. Lett.* **17** 024026

View the article online for updates and enhancements.

You may also like

- Prospects for generating electricity by large onshore and offshore wind farms
Patrick J H Volker, Andrea N Hahmann, Jake Badger et al.
- Are global wind power resource estimates overstated?
Amanda S Adams and David W Keith
- Chemical Reaction Mechanism between A-Site Deficient La Substituted $SrTiO_3$ and $PH_3$ in Coal Syngas
Gang Chen, Haruo Kishimoto, Katsuhiko Yamaji et al.

This content was downloaded from IP address 163.9.11.189 on 16/03/2022 at 15:18

ENVIRONMENTAL RESEARCH
LETTERS

LETTER

# Impacts of 319 wind farms on surface temperature and vegetation in the United States

**Yingzuo Qin**[1,2], **Yan Li**[1,2,*], **Ru Xu**[1,2], **Chengcheng Hou**[1,2], **Alona Armstrong**[3,4], **Eviatar Bach**[5], **Yang Wang**[6] and **Bojie Fu**[2,7]

[1] State Key Laboratory of Earth Surface Processes and Resources Ecology, Faculty of Geographical Science, Beijing Normal University, Beijing 100875, People's Republic of China
[2] Institute of Land Surface System and Sustainable Development, Faculty of Geographical Science, Beijing Normal University, Beijing 100875, People's Republic of China
[3] Lancaster Environment Centre, Library Avenue, Lancaster University, Lancaster, LA1 4YQ, United Kingdom
[4] Energy Lancaster, Science & Technology Building, Lancaster University, Lancaster, LA1 4YF, United Kingdom
[5] Geosciences Department and Laboratoire de Météorologie Dynamique (CNRS and IPSL), École Normale Supérieure and PSL University, Paris, France
[6] National Climate Center, China Meteorological Administration, Beijing 100081, People's Republic of China
[7] State Key Laboratory of Urban and Regional Ecology, Research Center for Eco-Environmental Sciences, Chinese Academy of Sciences, Beijing 100085, People's Republic of China
[*] Author to whom any correspondence should be addressed.

**E-mail:** yanli.geo@gmail.com

**Keywords:** wind farm, temperature, vegetation, land cover, LST, NDVI

Supplementary material for this article is available online

OPEN ACCESS

RECEIVED
14 September 2021

REVISED
26 December 2021

ACCEPTED FOR PUBLICATION
10 January 2022

PUBLISHED
11 February 2022

Original content from this work may be used under the terms of the Creative Commons Attribution 4.0 licence.

Any further distribution of this work must maintain attribution to the author(s) and the title of the work, journal citation and DOI.

## Abstract

The development of wind energy is essential for decarbonizing energy production. However, the construction of wind farms changes land surface temperature (LST) and vegetation by modifying land surface properties and disturbing land–atmosphere interactions. In this study, we used moderate resolution imaging spectroradiometer satellite data to quantify the impacts on local climate and vegetation of 319 wind farms in the United States. Our results indicated insignificant impacts on LST during the daytime but significant warming of 0.10 °C of annual mean nighttime LST averaged over all wind farms, and 0.36 °C for those 61% wind farms with warming. The nighttime LST impacts exhibited seasonal variations, with stronger warming in winter and autumn, up to 0.18 °C, but weaker effects in summer and spring. We observed a decrease in peak normalized difference vegetation index (NDVI) for 59% of wind farms due to infrastructure construction, with an average reduction of 0.0067 compared to non-wind farm areas. The impacts of wind farms depended on wind farm size, with winter LST impacts for large and small wind farms ranging from 0.21 °C to 0.14 °C, and peak NDVI impacts ranging from −0.009 to −0.006. The LST impacts declined with the increasing distance from the wind farm, with detectable impacts up to 10 km. In contrast, the vegetation impacts on NDVI were only evident within the wind farm locations. Wind farms built in grassland and cropland showed larger warming effects but weaker vegetation impact than those built on forests. Furthermore, spatial correlation analyses with environmental factors suggest limited geographical controls on the heterogeneous wind farm impacts and highlight the important role of local factors. Our analyses based on a large sample offer new evidence for wind farm impacts with improved representativeness compared to previous studies. This knowledge is important to fully understand the climatic and environmental implications of energy system decarbonization.

## 1. Introduction

The deployment of renewable energy technologies has grown significantly in recent years and is expected to accelerate around the world. The goal of the Paris Agreement is to limit the average global mean temperature increase well below 2 °C relative to pre-industrial levels by 2100, and to pursue efforts

© 2022 The Author(s). Published by IOP Publishing Ltd

to limit the increase to 1.5 °C (UNFCCC 2015). To reduce the energy-associated greenhouse gas emissions, it is essential to substitute the use of fossil fuels (Amponsah *et al* 2014) with renewable energy resources (Saidur *et al* 2011). Wind energy has experienced significant growth and is anticipated to be one of the dominant sources of low-carbon electricity in the future; the global wind power electricity generation was 1405 TWh in 2019 and is projected to reach 4355 TWh by 2030 (IEA 2020). In the United States, wind-generated electricity reached 275 TWh in 2018 (Pryor *et al* 2020).

Despite the climate benefits of wind power, there is a growing concern about the environmental effects of the increased land use and land cover change for wind farms. For example, the large deployment of wind farms can adversely affect local animal habitats, and the rotary blades of wind turbines can kill birds (Bright *et al* 2008) and bats (Voigt *et al* 2012). Wind farm construction can also result in deforestation, soil erosion, and impacts on land carbon sequestration (Dai *et al* 2015, Armstrong *et al* 2016).

The modification of land surface properties by wind farms also strongly influences the local and regional climate (Kirk-Davidoff and Keith 2008, Baidya Roy and Traiteur 2010, Zhou *et al* 2012), which in turn will influence ecosystem processes (Armstrong *et al* 2016). Changes to the climate are attributable to the wind turbines increasing the surface roughness (Kirk-Davidoff and Keith 2008) with implications for turbulence (Xia *et al* 2016) and mixing in the atmospheric boundary layer (ABL) (Baidya Roy and Traiteur 2010). Moreover, the wind turbines remove energy from the system and decrease downstream wind speeds (Miller and Kleidon 2016). Localized warming caused by either enhanced vertical mixing of the ABL or the vertical convergence of turbulent heat flux below hub height (Archer *et al* 2019, Wu and Archer 2021) has been quantified for several wind farms. For example, wind farms in Texas (Zhou *et al* 2012) and Illinois (Slawsky *et al* 2015) have been reported to cause local nighttime warming of 0.72 °C and 0.18 °C–0.39 °C per decade respectively. The impacts of wind farms on daytime temperature are weaker (Zhou *et al* 2012, Xia *et al* 2016) and tend towards cooling. For example, daytime cooling was detected in San Gorgonio, California (Baidya Roy and Traiteur 2010).

Given the temperature regulation of ecosystem processes, climate impacts and land cover changes associated with wind farms could alter vegetation. To date, the impacts of wind farms on local vegetation are mixed with no consensus in the literature. There have been studies reporting negative impacts of wind farms on plant species diversity in the Dobrogea Region of Southeast Romania (Urziceanu *et al* 2021) and vegetation growth in Northern China (Tang *et al* 2017), while others found no detectable impacts (Xia *et al* 2016). However, positive impacts on vegetation were observed in the Gobi desert (Xu *et al* 2019), and simulations of large-scale wind farm deployment projected enhanced vegetation growth due to precipitation feedbacks in the Sahara (Li *et al* 2018).

The variation in the environmental impacts of wind farms reflects the heterogeneity of wind farm characteristics such as their spatial extent, density, and their background climate conditions. First, the climatic impacts of wind farms are scale-dependent because the size, density, height, and rotor diameter of wind turbines influence the perturbation on land surfaces and the atmosphere. When the spatial extent of wind farms becomes sufficiently large (e.g. spanning hundreds to thousands of $km^2$), their impacts may go beyond the local scale and trigger changes in regional and continental-scale climate (Zhang *et al* 2013). Second, the background climate conditions influence the climatic impacts of wind farms. For example, the ratio between turbulent kinetic energy (TKE) induced by wind farms and background TKE explains not only the day-night contrast of wind farm impact and the warming magnitude of nighttime land surface temperature (LST) but also the seasonal variations in nighttime LST changes (Baidya Roy and Traiteur 2010, Xia *et al* 2016).

Resolving the likely impacts of specific wind farms on the climate, and implications for vegetation and thereby ecosystem function, requires the assessment of controlling characteristics. *In-situ* measurements of meteorological variables such as wind velocity, temperature, and precipitation during the operation of wind turbines provide valuable information for monitoring the impacts (e.g. in the Midwestern US (Smith *et al* 2013) and Scotland (Armstrong *et al* 2016)), but these measurements are often limited to a short period or a single wind farm. Numerical simulation of the impacts with climate models reveals the dynamic interactions between wind farms and the atmosphere as well as their impacts on climate (Fitch *et al* 2013, Chatterjee *et al* 2016). However, uncertainties in climate models and wind farm parameterizations, as well as the expensive computation cost, limit their usage for informing wind farm impacts at fine scales. In contrast, the high spatial resolution and global coverage of satellite data such as moderate resolution imaging spectroradiometer (MODIS) and Landsat allow detection of changes in surface temperature and vegetation and have been widely used to assess wind farm impacts (Zhou *et al* 2013, Slawsky *et al* 2015).

Existing quantification efforts using satellite data have mainly focused on individual wind farm (Baidya Roy and Traiteur 2010, Zhou *et al* 2012, Harris *et al* 2014, Slawsky *et al* 2015, Tang *et al* 2017), making their results lack representativeness and precluding robust comparison. Hence, it is necessary to systematically analyze a large number of wind farms to investigate their impacts on local climate and vegetation, and the implications of wind farms' characteristics

and geographic distribution. Consequently, in this study, by using satellite data, we quantify the impacts of 319 wind farms on local surface temperature and vegetation in the United States, analyzing the spatial-temporal patterns, and exploring influencing factors driving the impacts.

## 2. Methods

### 2.1. Data

The wind farms dataset used in this study was the US Wind Turbines Dataset (https://eerscmap.usgs.gov/uswtdb/, accessed Feb 2020), which includes geographical location, construction year, and turbine capacity for more than 60 000 individual wind turbines in the United States. A Density-Based Spatial Clustering of Applications with Noise (DBSCAN) algorithm from the scikit-learn package in Python (Pedregosa *et al* 2011) was used to classify individual turbines into wind farm cluster if their distance from each other was smaller than 0.1 degrees. Clusters of less than five turbines or construction years later than 2018 were excluded from further analysis. This resulted in a total of 319 wind farms, which were divided into three groups by their sizes (i.e. the number of wind turbines): small ($\leqslant$25, $n = 108$), medium (26–75, $n = 106$), and large (>75, $n = 105$) (figure 1(a)). The construction year of wind farms was defined as the year the majority of the wind turbines were built.

The remotely sensed LST data product (MYD11A2.006) from MODIS Aqua was used to quantify the temperature impact. The LST dataset has a spatial resolution of 1 km and temporal resolution of 8 day from 2004 to 2018. The overpass time of Aqua (1:30 and 13:30) approximates the daily minimum and maximum temperature of a day. The normalized difference vegetation index (NDVI) from MODIS Aqua (MYD13A2.006), which has a spatial and temporal resolution of 1 km and 16 d, respectively, was used to quantify impacts on vegetation. LST and NDVI data from 2004 to 2018 were used. To explore factors influencing wind farm impacts, we used climate variables including 2 m surface temperature, precipitation, and wind velocity at 100 m from ERA-5 reanalysis data (Hersbach *et al* 2020) at a spatial resolution of 0.25°. Also, we used lapse rate to represent the near-surface atmospheric inversion condition (Baidya Roy and Traiteur 2010), calculated as the average vertical gradient of potential temperature between 975 and 1000 hPa pressure levels. Additionally, the land cover data from MODIS (MCD12Q1.006) at 1 km resolution in 2011 and digital elevation data from Shuttle Radar Topography Mission at 30 m resolution in 2004 were used.

### 2.2. Quantifying the impacts of wind farms

The impacts of wind farms were quantified by comparing the LST and NDVI between the wind farms (WFs) and nearby non-wind-farm (NWF) areas. The NWF reference areas were defined as the buffering zone 8–10 km away from the wind farm boundary (NWF8_10, figure 1(b)), assuming a minimal wind farm impact while excluding water pixels. Because wind farms can also affect downwind areas due to the 'spillover' effect (changes in land surface properties in one area affecting adjacent areas), we created 2 km wide NWF buffering zones at 2–4 km (NWF2_4), 4–6 km (NWF4_6), and 6–8 km (NWF6_8) away from the wind farm boundaries (figure 1(b)). The 0–2 km buffer zone was not used (Zhou *et al* 2012) because it is influenced by wind farms directly due to its close distance.

Impacts of the wind farms on LST were quantified as the differences between WFs and NWFs during a time window centered on the construction year of wind farms ($\Delta$LST) (equation (1)):

$$\Delta\,\mathrm{LST} = \Delta\mathrm{LST}_{\mathrm{WF}} - \Delta\mathrm{LST}_{\mathrm{NWF}} = \mathrm{LST}_{\mathrm{Trend}_{\mathrm{WF}}} \times \Delta T - \mathrm{LST}_{\mathrm{Trend}_{\mathrm{NWF}}} \times \Delta T \quad (1)$$

where $\Delta\mathrm{LST}_{\mathrm{WF}}$ and $\Delta\mathrm{LST}_{\mathrm{NWF}}$ are the temporal LST changes for WFs and NWF areas, respectively, which can be estimated by their linear trends ($\mathrm{LST}_{\mathrm{Trend}_{\mathrm{WF}}}$ and $\mathrm{LST}_{\mathrm{Trend}_{\mathrm{NWF}}}$) during the time window and then multiplied by the length of the time window ($\Delta T$). This equation assumes that at LST changes in WFs are affected by effects from both wind farm and natural climate variability. In contrast, LST changes in NWFs are only affected by natural climate variability. Since WFs and NWFs in close distance are assumed to share the same natural climate variability, subtracting these two could effectively remove natural climate variability and isolate the wind farm effect, and their differences are attributable to wind farms. Similarly, the impacts of wind farms on vegetation were quantified as the differences in peak NDVI (the 95th percentile of annual NDVI) between WF and NWF areas ($\Delta$NDVI) following equation (2):

$$\Delta\mathrm{NDVI} = \Delta\mathrm{NDVI}_{\mathrm{WF}} - \Delta\mathrm{NDVI}_{\mathrm{NWF}} = \mathrm{NDVI}_{\mathrm{Trend}_{\mathrm{WF}}} \times \Delta T - \mathrm{NDVI}_{\mathrm{Trend}_{\mathrm{NWF}}} \times \Delta T. \quad (2)$$

Here we selected 5 years as the time window (i.e. the construction year and 2 years before and after it) to estimate wind farm impacts. The 5 years were chosen to balance the length of the time window and the available wind farm samples. For example, the 5 year time window means that WFs built before 2004 or later than 2017 would be excluded because MODIS LST data were available from 2002 until 2019. Figure 1(b) provides a wind farm example in Colorado built in 2015 to illustrate the quantification of wind farm impacts on LST. The LST of WF had a larger warming trend (0.14 °C $\mathrm{yr}^{-1}$) than NWF (0.06 °C $\mathrm{yr}^{-1}$) during the 5 year window, which

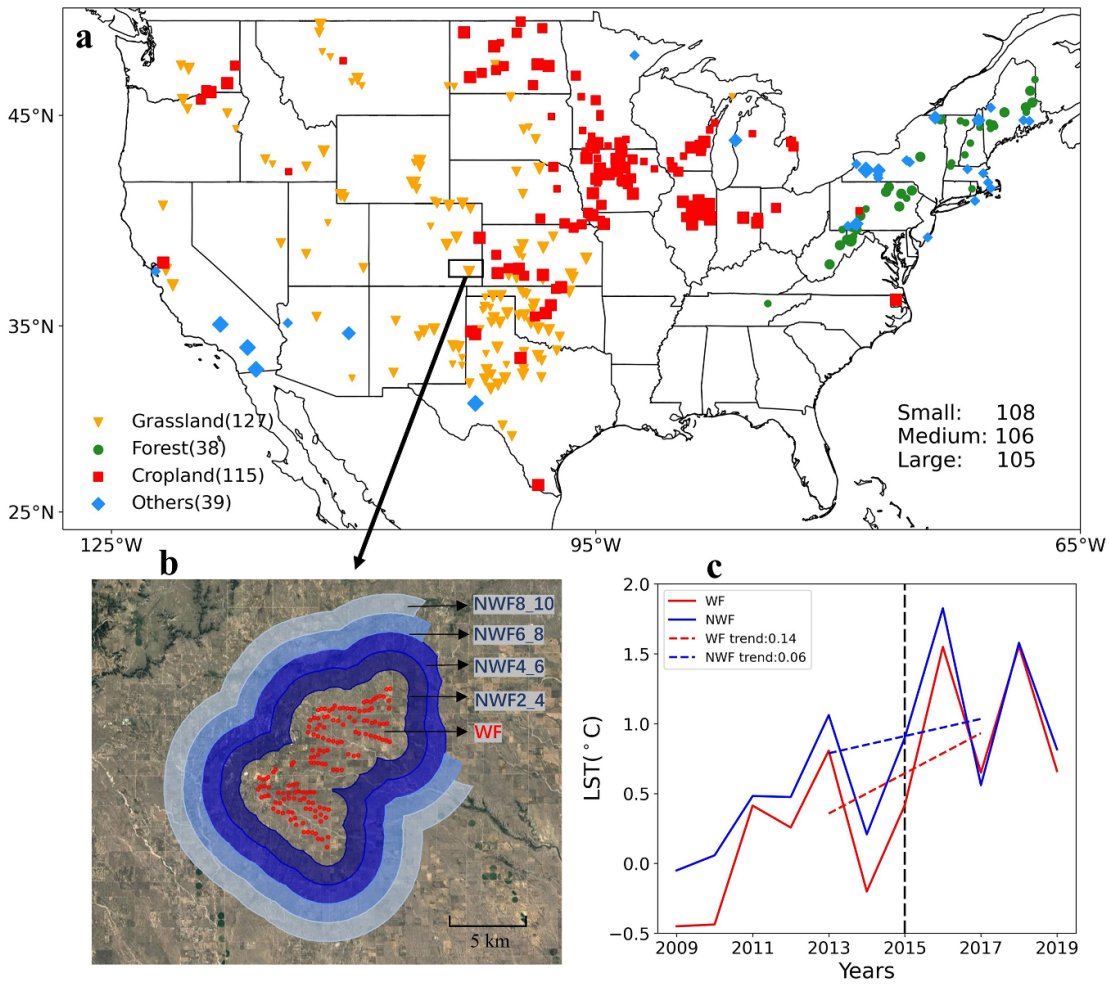



**Figure 1.** Diagram of quantifying impacts of 319 wind farms in the US. (a) The spatial distribution of 319 wind farms and their land cover types. (b) A wind farm sample in Colorado (104.23° W, 39.02° N). Red points denote individual wind turbines of the wind farm (WF) areas. The belts denote non–wind farm (NWF) areas defined by 2 km width buffer zones created with different distances to wind farms, including 2–4 km (NWF2_4), NWF4_6, NWF6_8, and NWF8_10. The missing parts of belts are the overlaps with adjacent wind farms. (c) Time series of annual nighttime LST for WF (solid red line) and NWF8_10 (solid blue line) from 2009 to 2019. The vertical black dotted line shows the construction year of the wind farm in 2015. The blue and red dashed lines are fitted linear trend lines of LST for WF and NWF. From 2013 to 2017, the LST trend (0.14 °C $yr^{-1}$) of WFs was larger than NWF (0.06 °C $yr^{-1}$), which indicates the warming impacts of wind farms on surface temperature.

translated to ΔLST of 0.40 °C, indicating the warming effects of wind farm (figure 1(c)).

## 3. Results

### 3.1. Wind farm impacts on surface temperature

Figure 2 shows the impacts of wind farms on annual mean daytime and nighttime LST in the US. During the daytime, the impact on LST showed random spatial patterns with mixed signs. The proportions of warming (ΔLST > 0) and cooling (ΔLST < 0) effects were about the same (49.84% vs. 50.16%) of all wind farm samples. The averaged daytime ΔLST of 319 wind farms was merely 0.01 ± 0.74 °C (mean ± 1 STD), and it did not pass the *t*-test ($p > 0.05$) (figure 2(a)), suggesting that wind farms did not produce a significant impact on daytime LST. However, 61.13% of wind farms showed warming effects at night, a percentage significantly more than the samples with cooling effects (38.87%). The averaged ΔLST at night of all samples was a significant warming effect of 0.10 ± 0.45 °C ($p < 0.01$), and it was 0.36 ± 0.32 °C for warming samples only which were mostly located in the Midwest of the US (figure 2(b)). These results indicated that wind farms had significant warming effects at night but weak or insignificant effects during the daytime.

To explore seasonality, we calculated ΔLST for spring (March to May), summer (July to August), autumn (September to November), and winter (December to February), respectively. During the daytime, the averaged ΔLST of all samples were insignificant for all four seasons ($p > 0.05$), with a proportion of warming and cooling samples fluctuating around 50% (figure S1 available online at stacks.iop.org/ERL/17/024026/mmedia). Because of the weak daytime effect, we mainly focused on the

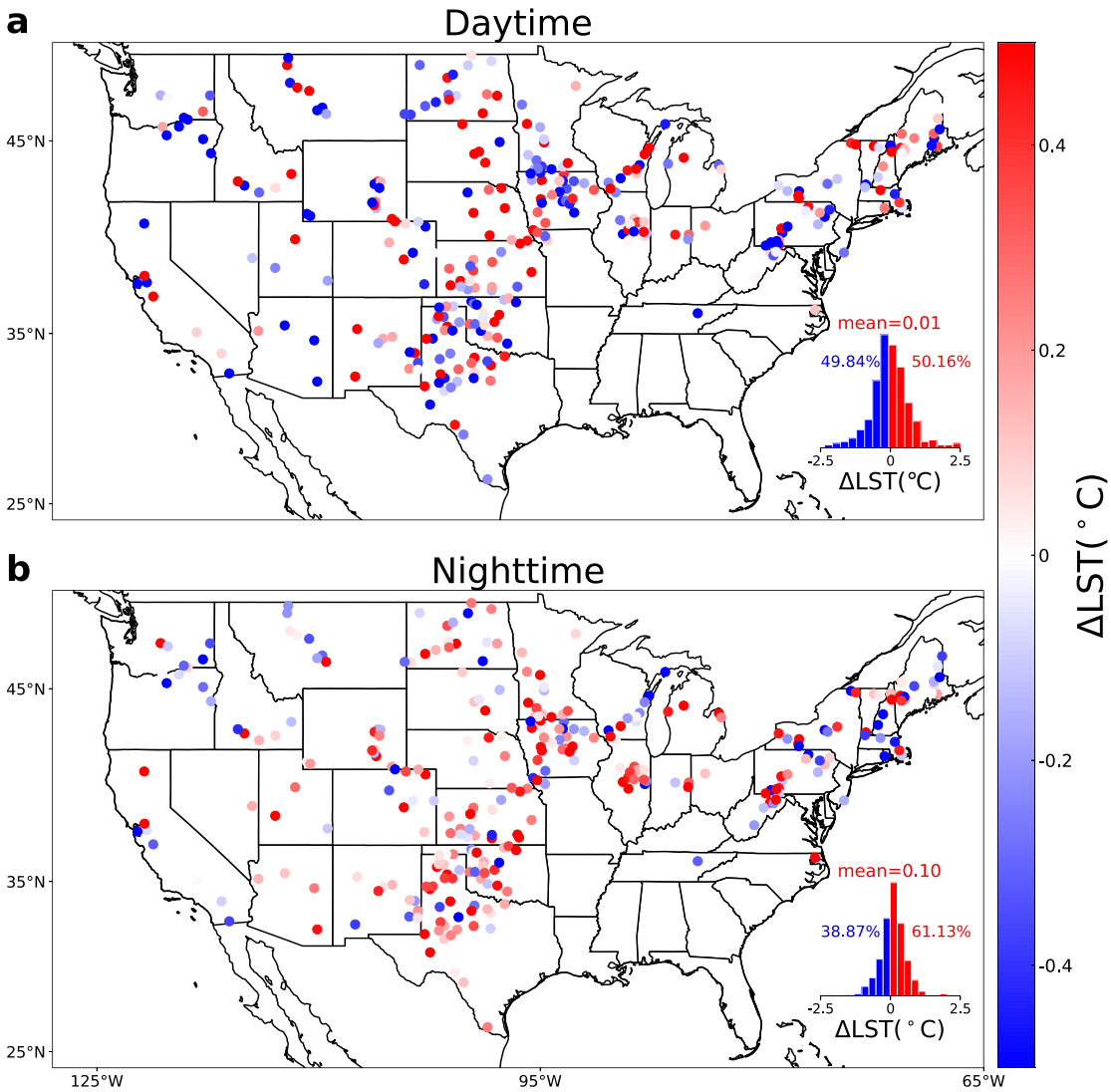



**Figure 2.** Wind farm impacts on annual mean daytime (a) and nighttime LST (b) (ΔLST). The insets show the histogram of ΔLST for 319 wind farms with mean values and percentages of positive (red) and negative (blue) values.

nighttime effects in the following analysis if not specified. During the nighttime, warming effects dominated all four seasons (figure 3), with the proportions of warming samples varying from 55.80% in winter to 63.64% in summer. In terms of the magnitude of ΔLST, strong night warming appeared in winter ($0.18 \pm 1.35$ °C, $p < 0.05$) and autumn ($0.16 \pm 0.73$ °C, $p < 0.01$), followed by summer (0.06 °C), and a slight cooling in spring (−0.02 °C). This is also supported by seasons with maximum and minimum LST impacts (figure 3(f)). The maximum nighttime effects occurred in winter for 44.20% of wind farm samples and in autumn for 24.14%, while the minimum effects occurred in summer for 41.69% and spring for 21.32% of samples. The mean seasonal ΔLST effect depends on both the relative frequency of warming and cooling samples, as well as the magnitude of the effects at each sample. The strong night warming effects in autumn and winter were due to a larger percentage of warming samples as well as a greater magnitude of ΔLST. The weak warming effects in spring and summer were mainly due to the small magnitude of ΔLST, although more wind farm samples showed warming effects.

### 3.2. Wind farm impacts on local vegetation

Wind farm impacts on local vegetation were quantified by the differences in peak NDVI (the 95th percentile of 16 d NDVI) between WFs and NWF areas (ΔNDVI, see equation (2)). Results in figure 4 show a widespread decrease in peak NDVI in WFs relative to NWFs, accounting for 59.25% of wind farm samples. The averaged ΔNDVI of 319 wind farms was $-0.007 \pm 0.042$ ($p < 0.01$) during the 5 year window. This demonstrates a negative impact on local vegetation, primarily due to vegetation clearing in the construction of wind farm infrastructure. The vegetation reduction caused by wind farms was also found in Bashang of Northern China (Tang *et al* 2017), reportedly due to suppressed soil moisture and enhanced water stress. However, about 40% of our wind farm samples did not decrease vegetation and

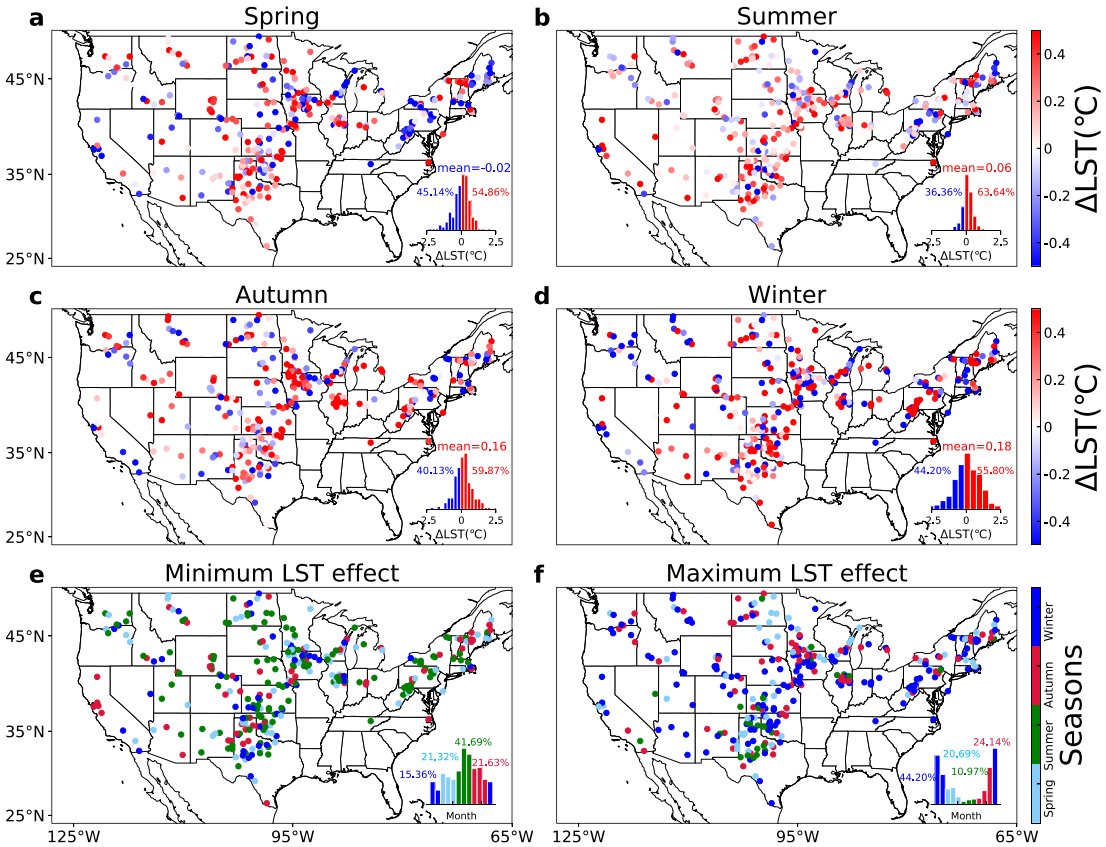



**Figure 3.** Seasonal variations of wind farm impacts on nighttime LST. Wind farm impacts on nighttime LST (ΔLST) in spring (a), summer (b), autumn (c), and winter (d). The months with minimum and maximum magnitude of ΔLST are shown in panels (e) and (f). The insets show the histogram of months with minimum and maximum magnitude of ΔLST.

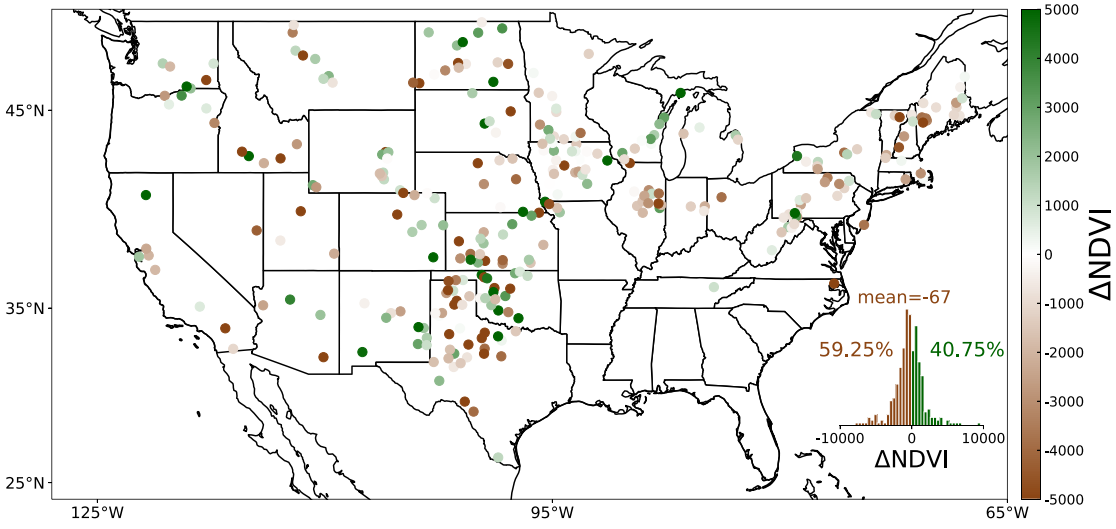



**Figure 4.** Wind farm impacts on peak NDVI (ΔNDVI). Note that the displayed NDVI values are multiplied by 10 000.

instead showed a higher peak NDVI. These results supported the possibility of non-detectable (Xia and Zhou 2017) or positive vegetation effects (Xu *et al* 2019) reported in other studies at an individual wind farm. Although the construction and operation of wind farms posed a negative impact on vegetation for most wind farms, such effects could be mitigated by other local factors. This revealed the complexity and variable effects of wind farms on vegetation.

### 3.3. Dependence of wind farm impacts on their size and distance

Wind farm impacts are expected to depend on the wind farm size and the distance away from wind

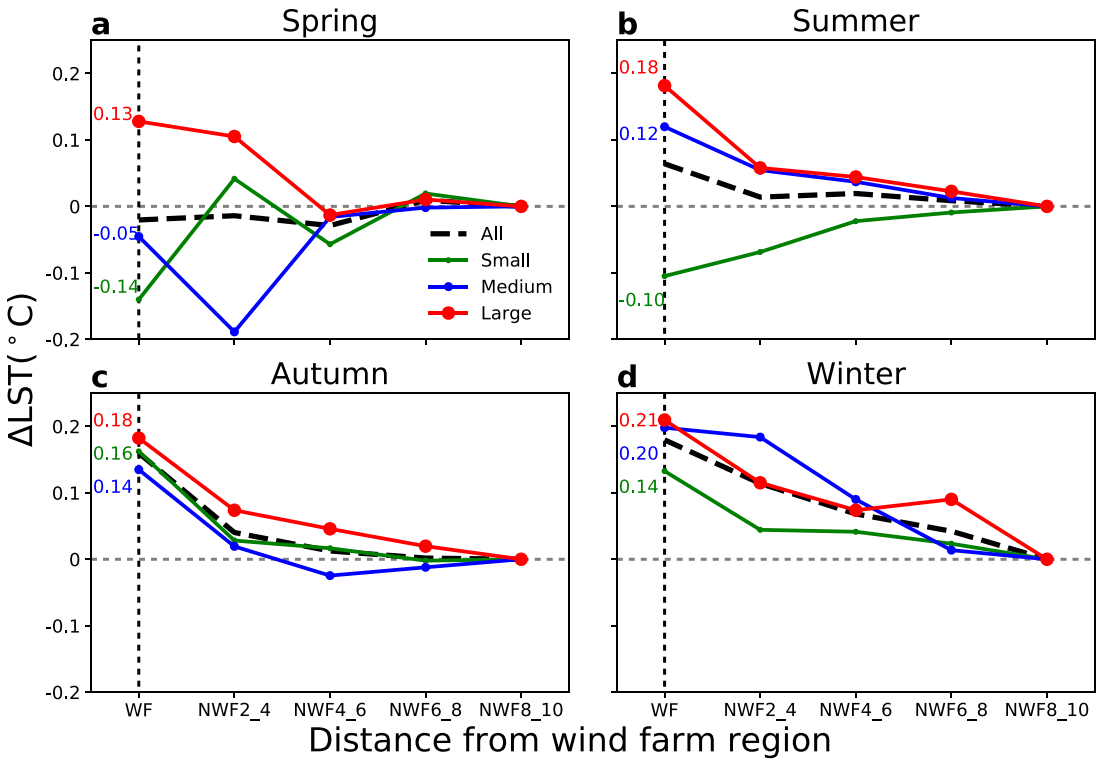



**Figure 5.** Influences of wind farm size and distance on nighttime ΔLST. Seasonal ΔLST is shown as a function of wind farm size and distance to wind farms. The small, medium, and large size wind farms are represented by lines of different colors. The dashed line represents all wind farm samples. NWF2_4, NWF4_6, NWF6_8, and NWF8_10 are NWF buffer areas with varying distances to WF areas (in km). ΔLST of WF is calculated as the LST differences between WF and the reference NWF areas NWF8_10. ΔLST of NWF2_4 is calculated as the LST differences between NWF2_4 and NWF8_10 following equation (1), and same for ΔLST of NWF4_6 and NWF6_8. The vertical dotted line highlights the WF area.

farms. To investigate these dependencies, we plotted the seasonal nighttime ΔLST of different farm sizes and their variations with different distances to wind farms. There was a general tendency for greater LST effects for larger wind farms (figure 5). For example, the warming effects in winter declined from 0.21 °C for large wind farms to 0.20 °C and 0.14 °C for medium and small farms, respectively (vertical lines in figure 5(d)). However, there were exceptions; the size dependence seems weaker for seasons with a small magnitude of ΔLST. In autumn, small farms exhibited a larger warming effect (0.16 °C) than medium farms (0.13 °C) because of the more intense warming of small farms over forests and cropland than that over medium farms (figure S2). In spring, when LST effects were weaker, only large wind farms exhibited warming while medium or small farms exhibited cooling at night.

Wind farm impacts on LST declined with increasing distance to wind farms, and the distance dependence was more evident in seasons or samples with a larger magnitude of ΔLST. In autumn and winter, the warming effects gradually decreased from 0.16 °C and 0.18 °C at WFs to zero at 8–10 km NWFs (the black dashed line in figure 5). This distance decay phenomenon of warming substantiates the 'spillover' effect because wind farm impacts extended much beyond their actual spatial coverage and affected LST in downstream areas (e.g. NWF2_4, NWF4_6, NWF6_8). The small or medium wind farms also had smaller footprints as their warming effects declined to zero at 4–6 km distance from wind farms. For spring and summer, when wind farm impacts were rather weak, such distance decay could be either absent or visible only for large farms. These results suggested an interactive effect of farm size and distance to wind farms.

Impacts of wind farms on vegetation (ΔNDVI) exhibited similar dependence on size and distance (figure 6(a)). At WFs, the negative impacts on vegetation were greatest in large farms, decreasing peak NDVI by 0.0085. The negative impacts were reduced to −0.006 for medium and small-sized wind farms. A stronger vegetation impact was expected for large wind farms because it involved the construction of more wind turbines than smaller-sized wind farms. Unlike the LST effects, which had a longer decay distance, the negative vegetation impacts disappeared at 2–4 km away from WFs, regardless of size. This indicated that the vegetation impacts of wind farms were mainly constrained to local scales and did not have detectable impacts on adjacent NWF regions.

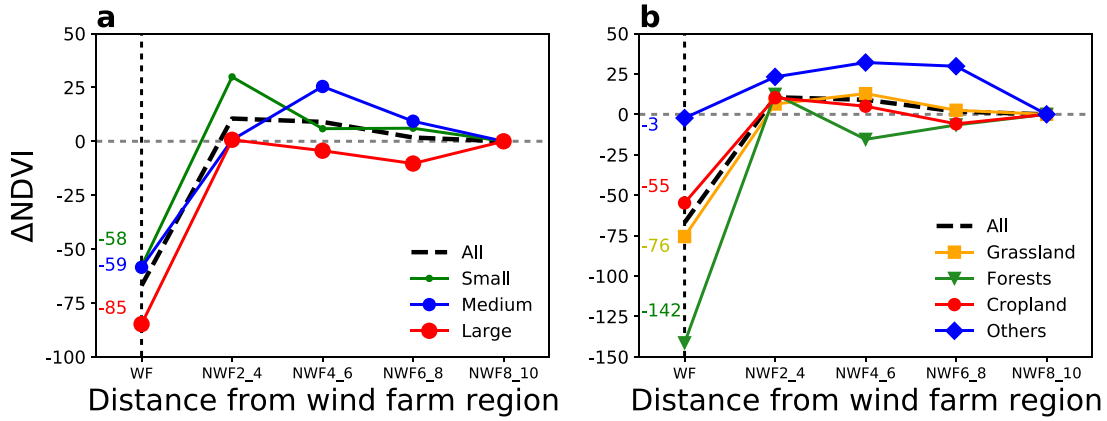



**Figure 6.** Influences of wind farm size (a), land cover (b), and distance to wind farms on ΔNDVI. (a) ΔNDVI is shown as a function of wind farm size and distance to wind farms. (b) ΔNDVI is shown as a function of land cover types and distance to wind farms. ΔNDVI of WF is calculated as the peak NDVI difference between WF and reference NWF areas NWF8_10 following equation (2). ΔNDVI of NWF2_4 is calculated as the peak NDVI differences between NWF2_4 and NWF8_10, and the same for ΔNDVI of NWF4_6 and NWF6_8. The vertical dotted line highlights the WF area. Note that the displayed NDVI values are multiplied by 10 000.

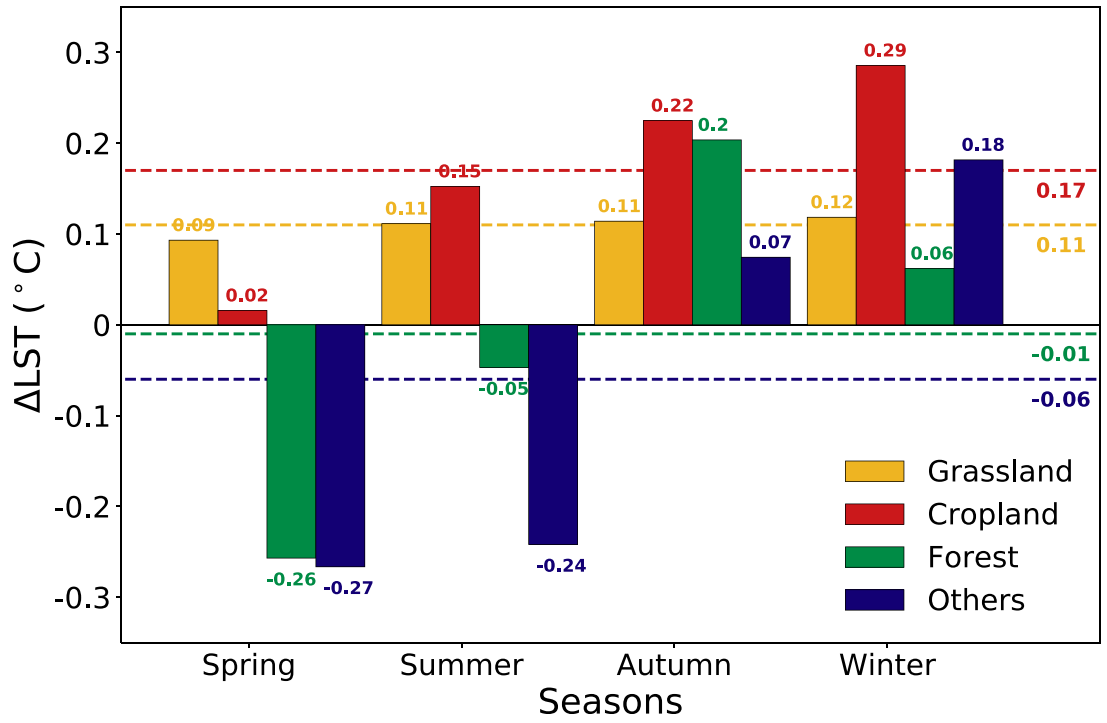



**Figure 7.** Influences of land cover type on nighttime ΔLST. Seasonal ΔLST is shown in the bar chart as a function of land cover types (grassland, forests, cropland, and others). The annual mean ΔLST of different land cover types is shown by horizontal dashed lines.

### 3.4. Dependence of wind farm impacts on land cover type

Since different land cover types have distinctive biophysical properties, wind farms built in different land cover types could have different impacts on LST and vegetation. We separated seasonal ΔLST into grassland, cropland, forest, and other land covers (figure 7). Wind farms in grassland and cropland had persistent nighttime warming effects in four seasons, with larger ΔLST in cropland (0.17 °C, ranging from 0.02 °C to 0.29 °C) than grassland (0.11 °C, ranging from 0.10 °C to 0.12 °C). This explains the mostly nighttime warming effects found in the central US where most wind farms were built in grassland (figure 1). In contrast, wind farms in forests and other land cover types, which mainly located in the northeast of the US, caused cooling in spring and summer (−0.27 °C to −0.05 °C), warming in autumn and winter (0.07 °C–0.20 °C), and consequently a slight annual cooling (−0.01 °C). It is worth noting that wind farms in forests were mainly small-sized farms (31 turbines on average), which means their LST

**Table 1.** Summary of research on wind farm impacts on surface temperature in the US and comparison with this study. Note that different studies adopted different quantification methods. Wind farm impact in Texas (Zhou *et al* 2012) and Illinois (Slawsky *et al* 2015) was quantified over a decade, and in Iowa's (Harris *et al* 2014) was quantified by the difference between mean states before and after the wind farm construction.

| | | Literature[a] | | This study | |
|---|---|---|---|---|---|
| Wind farm | Season | Daytime | Nighttime | Daytime | Nighttime |
| Texas[1] | Summer | −0.037 °C decade$^{-1}$ | 0.724 °C decade$^{-1}$ | 0.22 °C | 0.29 °C |
| | Winter | 0.233 °C decade$^{-1}$ | 0.458 °C decade$^{-1}$ | −0.13 °C | 0.16 °C |
| Illinois[2] | Summer | No apparent impacts | 0.18 °C decade$^{-1}$ | 0.59 °C | 0.24 °C |
| | Winter | | 0.39 °C decade$^{-1}$ | 0.22 °C | 0.86 °C |
| Iowa[3] | Spring | No apparent impacts | 0.037 °C | −0.03 °C | 0.18 °C |
| (a) | Summer | | 0.184 °C | 0.22 °C | 0.29 °C |
| | Autumn | | 0.202 °C | −0.58 °C | 0.21 °C |
| Iowa[3] | Spring | | −0.093 °C | 0.47 °C | 0.46 °C |
| (b) | Summer | | 0.227 °C | −0.48 °C | 0.67 °C |
| | Autumn | | 0.181 °C | −0.51 °C | 0.35 °C |
| Iowa[3] | Spring | | 0.152 °C | −1.90 °C | 0.06 °C |
| (c) | Summer | | 0.119 °C | 0.05 °C | −0.01 °C |
| | Autumn | | 0.181 °C | 0.90 °C | 0.27 °C |
| Iowa[3] | Spring | | 0.213 °C | 0.42 °C | 0.00 °C |
| (d) | Summer | | 0.143 °C | 0.02 °C | 0.19 °C |
| | Autumn | | 0.238 °C | 0.27 °C | 0.51 °C |
| Iowa[3] | Spring | | 0.356 °C | −0.52 °C | −0.74 °C |
| (e) | Summer | | 0.259 °C | 0.14 °C | 0.17 °C |
| | Autumn | | 0.485 °C | −1.70 °C | 0.34 °C |

[a] References for the three compared wind farms include 1. Texas (Zhou *et al* 2012), 2. Illinois (Slawsky *et al* 2015), and 3. Iowa (Harris *et al* 2014).

impacts in spring and summer were rather weak and could be disturbed by other local factors (figure 5(a)).

As for ΔNDVI, the vegetation decrease was the largest in wind farms built in the forests (−0.014), followed by grassland (−0.008) and cropland (−0.006) (figure 6(b)). This pattern probably reflected the fact that forests had higher NDVI than grassland and cropland. Therefore, vegetation disturbance induced by wind farm infrastructure would cause larger changes over forests.

## 4. Discussion

Our analyses based on a large sample of wind farms in the US revealed the prominent warming effects of wind farms at night but undetectable effects during the daytime. Though there are still debates on the mechanism of wind farm impacts on LST, the diurnal asymmetry effects can be explained by the differences in ABL stability. Under a stable ABL, which typically formed at night (i.e. warm air above cold air), wind turbine enhances vertical mixing and brings the much warmer air aloft to the bottom layer, leading to local warming effects (Baidya Roy and Traiteur 2010, Zhou *et al* 2012, Harris *et al* 2014, Armstrong *et al* 2016, Xia *et al* 2016). However, a recent field campaign pointed out that the near-surface warming could be caused by heat flux convergence below the rotor (Archer *et al* 2019, Wu and Archer 2021). During the daytime, when the ABL is unstable, and the air is well-mixed due to solar heating, combined with high background TKE (Xia *et al* 2016), wind turbines do not have a significant effect.

The 319 wind farms used here provide a more comprehensive assessment and improve the representativeness of earlier research that focused on individual wind farm. Therefore, our study reproduced previous findings at a few wind farms and expanded to more farms whose impacts have not been quantified before. For example, the significant nighttime warming found in Texas (Zhou *et al* 2012) and stronger winter warming effects in Illinois (Slawsky *et al* 2015) are consistent with our study (table 1). Although the wind farm in Texas (Zhou *et al* 2012) reported larger warming in summer than winter, our results indicated that only about 10% of wind farm samples followed this seasonal pattern (figure 3). For 68.34% of samples, the maximum impact occurred in autumn and winter during the nighttime. This shows that our results can better capture the climatic impacts of wind farms and reconcile inconsistent results reported in the literature.

As for impacts on vegetation, our results showed decreased vegetation for most wind farms, especially those large farms. However, positive and insignificant impacts were observed as well. The decreased vegetation is mainly caused by the construction of wind farms and the associated land cover changes, limiting vegetation growth in wind farms (Tang *et al* 2017, Urziceanu *et al* 2021). The increased vegetation in wind farms may be caused by the changing microclimate conditions induced by wind farms. For example,

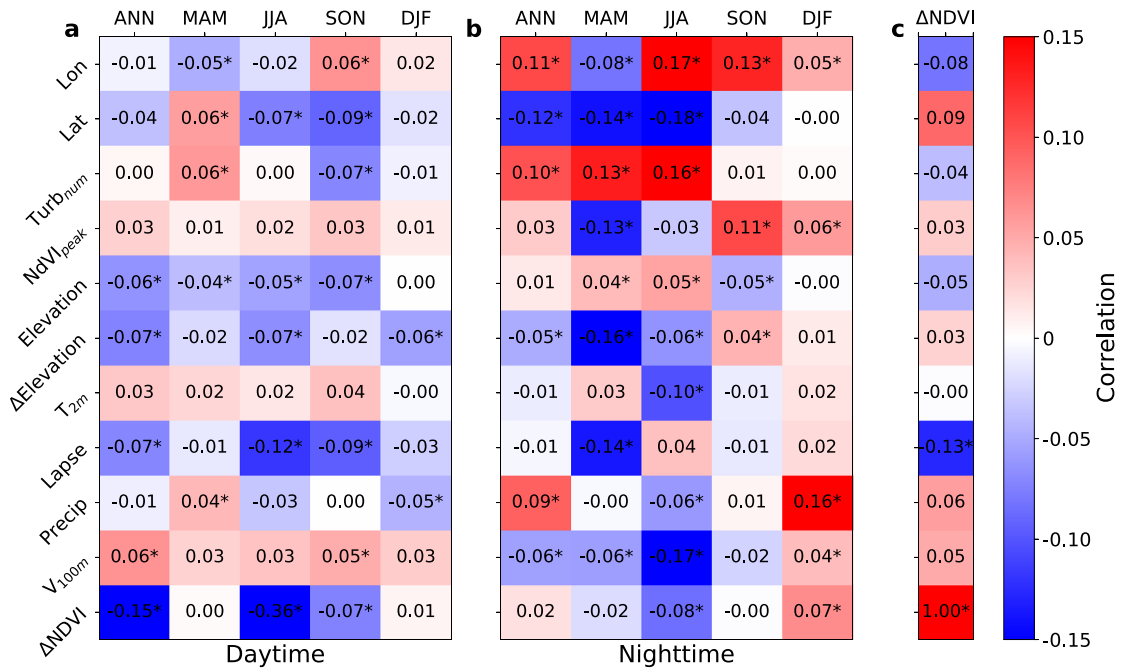



**Figure 8.** Spatial correlations between environmental factors and ΔLST (a), (b) and ΔNDVI (c). Environmental variables include longitude (Lon), latitude (Lat), turbine numbers ($Turb_{num}$), annual peak NDVI ($NDVI_{peak}$), elevation (Elevation), elevation difference (ΔElevation) between WFs and NWF region, annual mean 2 m temperature ($T_{2m}$), lapse rate (Lapse), precipitation (Precip), and 100 m wind velocity ($V_{100m}$) derived from ERA5. Numbers with asterisks indicate statistical significance ($p < 0.05$) as calculated using a *t*-test.

the downwind wake effect could reduce evapotranspiration (ET) and drought stress in the Gobi Desert, China (Xu *et al* 2019). The upwind and downwind regions of wind farms could cause different impacts (Meyers and Meneveau 2012), but we did not distinguish them in our analyses. There is evidence for undetectable impacts of wind farms on vegetation growth in west-central Texas (Xia and Zhou 2017). Hence, the impacts of wind farms on local vegetation are complex and variable, which are influenced by human activity, altered local climate, or any other undiscovered local factors.

The large spatial variability in the wind farm impacts reflects the combined effects of wind farm characteristics and environmental conditions. We found that the climatic impacts of wind farms depend on farm size and its underlying land cover. Lager wind farms caused greater changes in roughness and other land surface properties (Barrie and Kirk-Davidoff 2010, Fitch *et al* 2013), making a stronger impact on surface temperature. The dependence on land cover types reflects different interactions between vegetation properties and LST. Forests have much higher roughness than grass and cropland; therefore, wind farms built in forests lead to smaller roughness changes and consequently weaker ΔLST. Compared with wind farms in grassland, wind farms built in cropland exhibited the strongest warming effects in winter. Wind farms in cropland are mainly located in the northern regions with frequent snow in winter. Due to the high albedo of snow, cropland covered by snow has a much lower LST than wind farms, which might enhance the LST contrast and, therefore, the warming effect of wind farms. Nonetheless, this explanation is mixed with the influence of other characteristics of wind farms. For example, wind farms built in forests were typically small farms. Moreover, the varying strength of ET among vegetation types (Bonan 2001) and irrigation cooling in cropland (Kueppers *et al* 2007) could also contribute to the different effects among different land covers.

To better understand the drivers of the spatial variations of wind farm impacts on LST, we collected multiple possible influencing factors and calculated their spatial correlations with ΔLST (figures 8(a) and (b)). Influence factors considered include temperature, precipitation, wind velocity, and lapse rate. Correlations with these factors were small, but nighttime ΔLST showed overall higher and more significant correlations ($p < 0.05$) than daytime ΔLST. The weak correlations with daytime ΔLST and their seasonally varying signs suggest that the chosen environmental factors could not well explain the spatial variations in the daytime ΔLST. This again confirms the insignificant impacts of wind farms on daytime LST. However, the daytime ΔLST in summer was found to be related to the vegetation impact of wind farms (ΔNDVI, $r = -0.36$), which was not found for nighttime ΔLST. This indicates that decreased vegetation in wind farm areas could lead to a daytime warming effect, while increased vegetation could lead to a

**Table 2.** Sensitivity of annual nighttime ΔLST to different time windows.

| Method | ΔLST in different time windows | | | ΔLST with alternative method[a] |
|---|---|---|---|---|
| Time window | 5 years | 7 years | 9 years | Variable |
| Wind farm number | 319 | 300 | 261 | 319 |
| Mean ΔLST (°C) | 0.10 | 0.10 | 0.07 | 0.07 |
| Warming (ΔLST > 0) | 61.13% | 68.00% | 68.20% | 63.60% |
| Cooling (ΔLST < 0) | 38.87% | 32.00% | 31.80% | 36.40% |

[a] ΔLST with alternative method is calculated as the difference between the mean states before and after the construction year (Harris *et al* 2014).

daytime cooling effect, reflecting the ET cooling effect of vegetation. In contrast, there were a few significant correlations ($p < 0.05$) with nighttime ΔLST, implying some geographical controls. For example, the significant correlations with latitude (negative) and longitude (positive) revealed a spatial gradient of larger night warming from south to north and from west to east of the US. There was also a tendency for higher nighttime ΔLST in regions with higher precipitation. Moreover, wind farm size (the number of wind turbines) was positively correlated with nighttime ΔLST, indicating greater warming effects for large wind farms. The elevation difference between WFs and NWF may also play a role. Nighttime warming tends to be larger when WFs are located at a lower elevation than NWFs, because temperature decreases with increasing altitude. Generally, it seems that the selected environmental variables are not key drivers of the spatial variations of wind farm impacts on LST. Further analysis is needed to investigate the influence of other undocumented local factors on the spatial pattern of ΔLST.

Our method for quantifying wind farm impacts contains uncertainties and limitations. Firstly, the MODIS satellite data have uncertainty. To reduce the uncertainty from a specific dataset, we compared the wind farm impacts on annual mean nighttime LST (Aqua: MYD11A2.006, Terra: MOD11A2.006), peak NDVI and peak enhanced vegetation index (Aqua: MYD13A2.006, Terra: MOD13A2.006) based on MODIS Aqua and Terra satellites. Similar results across datasets in table S1 support the dominance of night warming and negative vegetation impacts of wind farms, demonstrating that our results are reliable. As described in section 2.2, we applied a 5 year time window (2 years before and after the construction year) to estimate ΔLST and ΔNDVI between WFs and NWFs based on their trend differences to reduce the influence of interannual temperature variability. The time window was chosen to balance the number of available wind farm samples since longer time windows filter out samples whose construction year was close to the beginning or end of the study period (table 2). Apart from the difference in trend, an alternative quantification method is to calculate the mean difference in LST or NDVI between two periods (3 years) before and after the construction year, whose results were comparable to our method (table 2). Moreover, the estimated impacts of a single wind farm could be influenced by the 'spillover' effect from nearby wind farms if they were too close. For simplicity, we assigned a single construction year for wind farms. The construction of wind farms may span several years, with new wind turbines installed each year. Besides, the downwind wakes produced by wind farms (Archer *et al* 2019) can also manifest their temperature effects in the multiple NWF buffering zones (from NWF2_4 to NWF8_10) and therefore contribute to the spillover effect. However, the wind farm impacts in our study only refer to local climate impacts, while the nonlocal impacts beyond 10 km from wind farms are not considered (Luo *et al* 2021).

## 5. Conclusion

Based on satellite remote sensing data, our assessment of 319 wind farms in the United States provides new observational evidence for the impacts of wind farms on local climate and vegetation. Our study reconciles the inconsistent impacts reported in previous studies, which focused only on a few individual wind farms lacking representativeness. Our results from a large sample of wind farms revealed significant local warming effects at night, insignificant impacts during the daytime, and the mostly negative impacts on vegetation. The large heterogeneity in wind farm impacts highlights the role of wind farm characteristics, environmental factors, and undocumented local factors. The quantification method can be applied to other countries or regions with available wind farm information. Further studies using satellite data at finer resolution than MODIS data could reveal the impact with more spatial detail. These observations can be combined with numerical simulations to advance the mechanistic understanding of wind farm impacts on the local climate. The improved knowledge of wind farm impacts helps inform the environmental consequences of wind energy development and guide clean energy planning for sustainable development.

## Data availability statement

All data used in this study are publicly available. The wind turbines database is obtained from the

US Wind Turbine Database (https://eerscmap.usgs.gov/uswtdb/). The code and data that support the findings of this study are openly available at the following URL/DOI: https://doi.org/10.6084/m9.figshare.17058272.

## Acknowledgments

This research is funded by the National Natural Science Foundation of China (No. 41901115) and the Fundamental Research Funds for the Central Universities. AA was supported by a Natural Environment Research Council, UK, Industrial Innovation Fellowship (NE/R013489/1). We thank Dr Xianghui Kong for providing suggestions on the earlier version of the work.

## Author contribution

Y L and Y Q conceived and designed the study; Y Q performed the data analysis. Y Q and Y L wrote the manuscript with contributions from A A, E B, R X, C H, Y W and B F. Y L and R X helped the data processing and analysis.

## ORCID iDs

Yingzuo Qin https://orcid.org/0000-0002-9802-0733
Yan Li https://orcid.org/0000-0002-6336-0981
Ru Xu https://orcid.org/0000-0002-5203-5980
Alona Armstrong https://orcid.org/0000-0001-8963-4621
Eviatar Bach https://orcid.org/0000-0002-9725-0203

## References

Amponsah N Y, Troldborg M, Kington B, Aalders I and Hough R L 2014 Greenhouse gas emissions from renewable energy sources: a review of lifecycle considerations *Renew. Sustain. Energy Rev.* **39** 461–75

Archer C L, Wu S, Vasel-Be-Hagh A, Brodie J F, Delgado R, St. Pé A, Oncley S and Semmer S 2019 The VERTEX field campaign: observations of near-ground effects of wind turbine wakes *J. Turbul.* **20** 64–92

Armstrong A, Burton R R, Lee S E, Mobbs S, Ostle N, Smith V, Waldron S and Whitaker J 2016 Ground-level climate at a peatland wind farm in Scotland is affected by wind turbine operation *Environ. Res. Lett.* **11** 044024

Baidya Roy S and Traiteur J J 2010 Impacts of wind farms on surface air temperatures *Proc. Natl Acad. Sci.* **107** 17899–904

Barrie D B and Kirk-Davidoff D B 2010 Weather response to a large wind turbine array *Atmos. Chem. Phys.* **10** 769–75

Bonan G B 2001 Observational evidence for reduction of daily maximum temperature by croplands in the Midwest United States *J. Clim.* **14** 2430–42

Bright J, Langston R, Bullman R, Evans R, Gardner S and Pearce-Higgins J 2008 Map of bird sensitivities to wind farms in Scotland: a tool to aid planning and conservation *Biol. Conserv.* **141** 2342–56

Chatterjee F, Allaerts D, Blahak U, Meyers J and van Lipzig N P M 2016 Evaluation of a wind-farm parametrization in a regional climate model using large eddy simulations *Q. J. R. Meteorol. Soc.* **142** 3152–61

Dai K, Bergot A, Liang C, Xiang W and Huang Z 2015 Environmental issues associated with wind energy—a review *Renew. Energy* **75** 911–21

Fitch A C, Olson J B and Lundquist J K 2013 Parameterization of wind farms in climate models *J. Clim.* **26** 6439–58

Harris R A, Zhou L and Xia G 2014 Satellite observations of wind farm impacts on nocturnal land surface temperature in Iowa *Remote Sens.* **6** 12234–46

Hersbach H *et al* 2020 The ERA5 global reanalysis *Q. J. R. Meteorol. Soc.* **146** 1999–2049

IEA 2020 Renewable power report *Int. Energy Assoc.* (available at: www.iea.org/reports/renewable-power)

Kirk-Davidoff D B and Keith D W 2008 On the climate impact of surface roughness anomalies *J. Atmos. Sci.* **65** 2215–34

Kueppers L M, Snyder M A and Sloan L C 2007 Irrigation cooling effect: regional climate forcing by land-use change *Geophy. Res. Let.* **34** 1–5

Li Y, Kalnay E, Motesharrei S, Rivas J, Kucharski F, Kirk-Davidoff D, Bach E and Zeng N 2018 Climate model shows large-scale wind and solar farms in the Sahara increase rain and vegetation *Science* **361** 1019–22

Luo L, Zhuang Y, Duan Q, Dong L, Yu Y, Liu Y, Chen K and Gao X 2021 Local climatic and environmental effects of an onshore wind farm in North China *Agric. For. Meteorol.* **308–9** 108607

Meyers J and Meneveau C 2012 Optimal turbine spacing in fully developed wind-farm boundary layers *Wind Energy* **15** 305–17

Miller L M and Kleidon A 2016 Wind speed reductions by large-scale wind turbine deployments lower turbine efficiencies and set low generation limits *Proc. Natl Acad. Sci. USA* **113** 13570–5

Pedregosa F, Varoquaux G and Gramfort A 2011 Scikit-learn: machine learning in Python *J. Mach. Learn.* **12** 2825–30

Pryor S C, Barthelmie R J and Shepherd T J 2020 20% of US electricity from wind will have limited impacts on system efficiency and regional climate *Sci. Rep.* **10** 1–14

Saidur R, Rahim N A, Islam M R and Solangi K H 2011 Environmental impact of wind energy *Renew. Sustain. Energy Rev.* **15** 2423–30

Slawsky L M, Zhou L, Roy S B, Xia G, Vuille M and Harris R A 2015 Observed thermal impacts of wind farms over Northern Illinois *Sensors* **15** 14981–5005

Smith C M, Barthelmie R J and Pryor S C 2013 *In situ* observations of the influence of a large onshore wind farm on near-surface temperature, turbulence intensity and wind speed profiles *Environ. Res. Lett.* **8** 034006

Tang B, Wu D, Zhao X, Zhou T, Zhao W and Wei H 2017 The observed impacts of wind farms on local vegetation growth in Northern China *Remote Sens.***9** 2011–3

UNFCCC 2015 Adoption of the Paris agreement (Geneva) (available at: https://unfccc.int/)

Urziceanu M, Anastasiu P, Rozylowicz L and Sesan T E 2021 Local-scale impact of wind energy farms on rare, endemic, and threatened plant species *Peer J.* **9** 1–22

Voigt C C, Popa-Lisseanu A G, Niermann I and Kramer-Schadt S 2012 The catchment area of wind farms for European bats: a plea for international regulations *Biol. Conserv.* **153** 80–86

Wu S and Archer C L 2021 Near-ground effects of wind turbines: observations and physical mechanisms *Mon. Weather Rev.* **149** 879–98

Xia G and Zhou L 2017 Detecting wind farm impacts on local vegetation growth in Texas and Illinois using MODIS vegetation greenness measurements *Remote Sens.* **9** 698

Xia G, Zhou L, Freedman J M, Roy S B, Harris R A and Cervarich M C 2016 A case study of effects of atmospheric boundary layer turbulence, wind speed, and stability on wind farm induced temperature changes using observations from a field campaign *Clim. Dyn.* **46** 2179–96

Xu K, He L, Hu H, Liu S, Du Y, Wang Z, Li Y, Li L, Khan A and Wang G 2019 Positive ecological effects of wind farms on vegetation in China's Gobi desert *Sci. Rep.* **9** 1–11

Zhang W, Markfort C D and Porté-Agel F 2013 Experimental study of the impact of large-scale wind farms on land–atmosphere exchanges *Environ. Res. Lett.* **8** 015002

Zhou L, Tian Y, Baidya Roy S, Thorncroft C, Bosart L F and Hu Y 2012 Impacts of wind farms on land surface temperature *Nat. Clim. Change* **2** 539–43

Zhou L, Tian Y, Chen H, Dai Y and Harris R A 2013 Effects of topography on assessing wind farm impacts using MODIS data *Earth Interact.* **17** 1–18